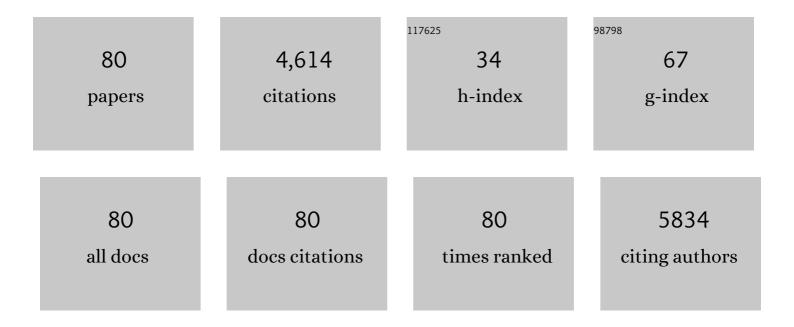
Laura Mezzanotte

List of Publications by Year in descending order

Source: https://exaly.com/author-pdf/3057012/publications.pdf Version: 2024-02-01



#	Article	IF	CITATIONS
1	Farnesyl Pyrophosphate Synthase Is the Molecular Target of Nitrogen-Containing Bisphosphonates. Biochemical and Biophysical Research Communications, 1999, 264, 108-111.	2.1	464
2	The Tumor Suppressor Smad4 Is Required for Transforming Growth Factor β–Induced Epithelial to Mesenchymal Transition and Bone Metastasis of Breast Cancer Cells. Cancer Research, 2006, 66, 2202-2209.	0.9	344
3	From The Cover: Murine malaria parasite sequestration: CD36 is the major receptor, but cerebral pathology is unlinked to sequestration. Proceedings of the National Academy of Sciences of the United States of America, 2005, 102, 11468-11473.	7.1	283
4	In vivo imaging of transcriptionally active estrogen receptors. Nature Medicine, 2003, 9, 82-86.	30.7	273
5	The Role of Geranylgeranylation in Bone Resorption and Its Suppression by Bisphosphonates in Fetal Bone Explants In Vitro: A Clue to the Mechanism of Action of Nitrogen-Containing Bisphosphonates. Journal of Bone and Mineral Research, 1999, 14, 722-729.	2.8	216
6	Nitrogen-Containing Bisphosphonates Inhibit Isopentenyl Pyrophosphate Isomerase/Farnesyl Pyrophosphate Synthase Activity with Relative Potencies Corresponding to Their Antiresorptive Potenciesin Vitroandin Vivo. Biochemical and Biophysical Research Communications, 1999, 255, 491-494.	2.1	191
7	Nasal vaccination with N-trimethyl chitosan and PLCA based nanoparticles: Nanoparticle characteristics determine quality and strength of the antibody response in mice against the encapsulated antigen. Vaccine, 2010, 28, 6282-6291.	3.8	176
8	Interleukin-17: A New Bone Acting Cytokine In Vitro. Journal of Bone and Mineral Research, 1999, 14, 1513-1521.	2.8	150
9	Expression of Indian Hedgehog, Parathyroid Hormone-Related Protein, and Their Receptors in the Postnatal Growth Plate of the Rat: Evidence for a Locally Acting Growth Restraining Feedback Loop After Birth. Journal of Bone and Mineral Research, 2000, 15, 1045-1055.	2.8	135
10	Monitoring Metastatic Behavior of Human Tumor Cells in Mice with Speciesâ€Specific Polymerase Chain Reaction: Elevated Expression of Angiogenesis and Bone Resorption Stimulators by Breast Cancer in Bone Metastases. Journal of Bone and Mineral Research, 2001, 16, 1077-1091.	2.8	117
11	Structural requirements for bisphosphonate actions in vitro. Journal of Bone and Mineral Research, 1994, 9, 1875-1882.	2.8	117
12	Dose-dependent effects of phytoestrogens on bone. Trends in Endocrinology and Metabolism, 2005, 16, 207-213.	7.1	111
13	Click beetle luciferase mutant and near infrared naphthyl-luciferins for improved bioluminescence imaging. Nature Communications, 2018, 9, 132.	12.8	101
14	Urokinase-Receptor/Integrin Complexes Are Functionally Involved in Adhesion and Progression of Human Breast Cancer in Vivo. American Journal of Pathology, 2001, 159, 971-982.	3.8	97
15	Role of fibroblasts in the regulation of proinflammatory interleukin IL-1, IL-6 and IL-8 levels induced by keratinocyte-derived IL-1. Archives of Dermatological Research, 1996, 288, 391-398.	1.9	92
16	Sensitive Dual Color In Vivo Bioluminescence Imaging Using a New Red Codon Optimized Firefly Luciferase and a Green Click Beetle Luciferase. PLoS ONE, 2011, 6, e19277.	2.5	88
17	Dissociation of binding and antiresorptive properties of hydroxybisphosphonates by substitution of the hydroxyl with an amino group. Journal of Bone and Mineral Research, 1996, 11, 1492-1497.	2.8	84
18	Transition of healthy to diseased synovial tissue in rheumatoid arthritis is associated with gain of mesenchymal/fibrotic characteristics. Arthritis Research and Therapy, 2006, 8, R165	3.5	80

#	Article	IF	CITATIONS
19	Immunohistochemical investigations on the differentiation marker protein E11 in rat calvaria, calvaria celvaria cell culture and the osteoblastic cell line ROS 17/2.8. Histochemistry and Cell Biology, 1999, 111, 61-69.	1.7	70
20	Role of trimethylated chitosan (TMC) in nasal residence time, local distribution and toxicity of an intranasal influenza vaccine. Journal of Controlled Release, 2010, 144, 17-24.	9.9	61
21	Evaluating reporter genes of different luciferases for optimized <i>in vivo</i> bioluminescence imaging of transplanted neural stem cells in the brain. Contrast Media and Molecular Imaging, 2013, 8, 505-513.	0.8	60
22	Effect of Angiogenic and Antiangiogenic Compounds on the Outgrowth of Capillary Structures from Fetal Mouse Bone Explants. Laboratory Investigation, 2001, 81, 5-15.	3.7	54
23	Sclerostin and the regulation of bone formation: Effects in hip osteoarthritis and femoral neck fracture. Journal of Bone and Mineral Research, 2010, 25, 1867-1876.	2.8	54
24	First missense mutation in the SOST gene causing sclerosteosis by loss of sclerostin function. Human Mutation, 2010, 31, E1526-E1543.	2.5	52
25	Leukemia inhibitory factor inhibits osteoclastic resorption, growth, mineralization, and alkaline phosphatase activity in fetal mouse metacarpal bones in culture. Journal of Bone and Mineral Research, 1993, 8, 191-198.	2.8	51
26	Ceramic hydroxyapatite implants for the release of bisphosphonate. Bone and Mineral, 1994, 25, 123-134.	1.9	49
27	Nanobody-targeted photodynamic therapy induces significant tumor regression of trastuzumab-resistant HER2-positive breast cancer, after a single treatment session. Journal of Controlled Release, 2020, 323, 269-281.	9.9	49
28	A multi-modality platform to image stem cell graft survival in the naÃ ⁻ ve and stroke-damaged mouse brain. Biomaterials, 2014, 35, 2218-2226.	11.4	47
29	Interleukin 6/Wnt interactions in rheumatoid arthritis: interleukin 6 inhibits Wnt signaling in synovial fibroblasts and osteoblasts. Croatian Medical Journal, 2016, 57, 89-98.	0.7	46
30	In vitro and Ex vivo evidence that estrogens suppress increased bone resorption induced by ovariectomy or PTH stimulation through an effect on osteoclastogenesis. Journal of Bone and Mineral Research, 1995, 10, 1523-1530.	2.8	45
31	Emerging tools for bioluminescence imaging. Current Opinion in Chemical Biology, 2021, 63, 86-94.	6.1	44
32	Bioluminescent imaging: Emerging technology for non-invasive imaging of bone tissue engineering. Biomaterials, 2006, 27, 1851-1858.	11.4	43
33	IL-1α, IL-1β, IL-6, and TNF-α Steady-State mRNA Levels Analyzed by Reverse Transcription-Competitive PCR in Bone Marrow of Gonadectomized Mice. Journal of Bone and Mineral Research, 1998, 13, 185-194.	2.8	40
34	Integrins and osteoclastic resorption in three bone organ cultures: Differential sensitivity to synthetic arg-gly-asp peptides during osteoclast formation. Journal of Bone and Mineral Research, 1994, 9, 1021-1028.	2.8	40
35	A New Multicolor Bioluminescence Imaging Platform to Investigate NF-κB Activity and Apoptosis in Human Breast Cancer Cells. PLoS ONE, 2014, 9, e85550.	2.5	35
36	A Dual-Color Bioluminescence Reporter Mouse for Simultaneous in vivo Imaging of T Cell Localization and Function. Frontiers in Immunology, 2018, 9, 3097.	4.8	32

#	Article	IF	CITATIONS
37	pH-Channeling in Cancer: How pH-Dependence of Cation Channels Shapes Cancer Pathophysiology. Cancers, 2020, 12, 2484.	3.7	31
38	First Report on Ex Vivo Delivery of Paracrine Active Human Mesenchymal Stromal Cells to Liver Grafts During Machine Perfusion. Transplantation, 2020, 104, e5-e7.	1.0	30
39	Human CD46-transgenic mice in studies involving replication-incompetent adenoviral type 35 vectors. Journal of General Virology, 2006, 87, 255-265.	2.9	29
40	Red-shifted click beetle luciferase mutant expands the multicolor bioluminescent palette for deep tissue imaging. IScience, 2021, 24, 101986.	4.1	29
41	Detecting tumour-positive resection margins after oral cancer surgery by spraying a fluorescent tracer activated by gamma-glutamyltranspeptidase. Oral Oncology, 2018, 78, 1-7.	1.5	28
42	Necrosis avid near infrared fluorescent cyanines for imaging cell death and their use to monitor therapeutic efficacy in mouse tumor models. Oncotarget, 2015, 6, 39036-39049.	1.8	28
43	Disodium 1-hydroxy-3-(1-pyrrolidinyl)-propylidene-1,1-bisphosphonate (EB-1053) is a potent inhibitor of bone resorption in vitro and in vivo. Journal of Bone and Mineral Research, 1992, 7, 981-986.	2.8	26
44	In Vivo Bioluminescence Imaging of Murine Xenograft Cancer Models with a Red-shifted Thermostable Luciferase. Molecular Imaging and Biology, 2010, 12, 406-414.	2.6	26
45	Targeted nanoparticles for the non-invasive detection of traumatic brain injury by optical imaging and fluorine magnetic resonance imaging. Nano Research, 2016, 9, 1276-1289.	10.4	26
46	Bone Morphogenetic Protein 7 Inhibits Tumor Growth of Human Uveal Melanoma In Vivo. , 2007, 48, 4882.		24
47	Development of a New Hyaluronic Acid Based Redox-Responsive Nanohydrogel for the Encapsulation of Oncolytic Viruses for Cancer Immunotherapy. Nanomaterials, 2021, 11, 144.	4.1	23
48	Evaluation of NanoLuc substrates for bioluminescence imaging of transferred cells in mice. Journal of Photochemistry and Photobiology B: Biology, 2021, 216, 112128.	3.8	23
49	A novel luciferase fusion protein for highly sensitive optical imaging: from single-cell analysis to in vivo whole-body bioluminescence imaging. Analytical and Bioanalytical Chemistry, 2014, 406, 5727-5734.	3.7	22
50	Alternative delivery of a thermostable inactivated polio vaccine. Vaccine, 2015, 33, 2030-2037.	3.8	21
51	Evaluating Brightness and Spectral Properties of Click Beetle and Firefly Luciferases Using Luciferin Analogues: Identification of Preferred Pairings of Luciferase and Substrate for In Vivo Bioluminescence Imaging. Molecular Imaging and Biology, 2020, 22, 1523-1531.	2.6	21
52	Fate of Multimeric Oligomers, Submicron, and Micron Size Aggregates of Monoclonal Antibodies Upon Subcutaneous Injection in Mice. Journal of Pharmaceutical Sciences, 2016, 105, 1693-1704.	3.3	19
53	Design of a Variant of Vascular Endothelial Growth Factor-A (VEGF-A) Antagonizing KDR/Flk-1 and Flt-1. Laboratory Investigation, 2002, 82, 473-481.	3.7	18
54	Pre-clinical Evaluation of a Cyanine-Based SPECT Probe for Multimodal Tumor Necrosis Imaging. Molecular Imaging and Biology, 2016, 18, 905-915.	2.6	17

#	Article	IF	CITATIONS
55	Independent pathways in the modulation of osteoclastic resorption by intermediates of the mevalonate biosynthetic pathway: The role of the retinoic acid receptor. Bone, 2006, 38, 167-171.	2.9	16
56	Ultrasound-mediated gene delivery of naked plasmid DNA in skeletal muscles: A case for bolus injections. Journal of Controlled Release, 2014, 195, 130-137.	9.9	16
57	Endostatin's heparan sulfate-binding site is essential for inhibition of angiogenesis and enhances in situ binding to capillary-like structures in bone explants. Matrix Biology, 2005, 23, 557-561.	3.6	13
58	Development of a Three-Dimensional In Vitro Model for Longitudinal Observation of Cell Behavior: Monitoring by Magnetic Resonance Imaging and Optical Imaging. Molecular Imaging and Biology, 2010, 12, 367-376.	2.6	13
59	Oestrogenic Compounds Modulate Cytokine-induced Nitric Oxide Production in Mouse Osteoblast-like Cells. Journal of Pharmacy and Pharmacology, 2010, 51, 1409-1414.	2.4	11
60	The Necrosis-Avid Small Molecule HQ4-DTPA as a Multimodal Imaging Agent for Monitoring Radiation Therapy-Induced Tumor Cell Death. Frontiers in Oncology, 2016, 6, 221.	2.8	11
61	Optimized Longitudinal Monitoring of Stem Cell Grafts in Mouse Brain Using a Novel Bioluminescent/Near Infrared Fluorescent Fusion Reporter. Cell Transplantation, 2017, 26, 1878-1889.	2.5	11
62	NanoBiT System and Hydrofurimazine for Optimized Detection of Viral Infection in Mice—A Novel in Vivo Imaging Platform. International Journal of Molecular Sciences, 2020, 21, 5863.	4.1	10
63	Traumatic Brain Injury: Preclinical Imaging Diagnostic(s) and Therapeutic Approaches. Current Pharmaceutical Design, 2017, 23, 1909-1915.	1.9	9
64	In Vitro and in Vivo Endochondral Bone Formation Models Allow Identification of Anti-Angiogenic Compounds. American Journal of Pathology, 2003, 163, 157-163.	3.8	8
65	Targeting Nanomedicine to Brain Tumors: Latest Progress and Achievements. Current Pharmaceutical Design, 2017, 23, 1953-1962.	1.9	8
66	Identification of differentially expressed genes in a renal cell carcinoma tumor model after endostatin-treatment. Laboratory Investigation, 2004, 84, 1472-1483.	3.7	7
67	Efficient in vivo knock-down of estrogen receptor alpha: application of recombinant adenovirus vectors for delivery of short hairpin RNA. BMC Biotechnology, 2006, 6, 11.	3.3	7
68	In Vivo Non-Invasive Tracking of Macrophage Recruitment to Experimental Stroke. PLoS ONE, 2016, 11, e0156626.	2.5	7
69	Intraoperative MET-receptor targeted fluorescent imaging and spectroscopy for lymph node detection in papillary thyroid cancer: novel diagnostic tools for more selective central lymph node compartment dissection. European Journal of Nuclear Medicine and Molecular Imaging, 2022, 49, 3557-3570.	6.4	7
70	In Vivo Evaluation of Indium-111–Labeled 800CW as a Necrosis-Avid Contrast Agent. Molecular Imaging and Biology, 2020, 22, 1333-1341.	2.6	6
71	Necrosis binding of Ac-Lys0(IRDye800CW)-Tyr3-octreotate: a consequence from cyanine-labeling of small molecules. EJNMMI Research, 2021, 11, 47.	2.5	5
72	Near-Infrared Bioluminescence Imaging of Macrophage Sensors for Cancer Detection In Vivo. Frontiers in Bioengineering and Biotechnology, 2022, 10, .	4.1	4

#	Article	IF	CITATIONS
73	Development of a Multicolor Bioluminescence Imaging Platform to Simultaneously Investigate Transcription Factor NF-κB Signaling and Apoptosis. Methods in Molecular Biology, 2016, 1461, 255-270.	0.9	3
74	Dually Cross-Linked Core-Shell Structure Nanohydrogel with Redox–Responsive Degradability for Intracellular Delivery. Pharmaceutics, 2021, 13, 2048.	4.5	3
75	In Vivo Evaluation of Gallium-68-Labeled IRDye800CW as a Necrosis Avid Contrast Agent in Solid Tumors. Contrast Media and Molecular Imaging, 2021, 2021, 1-8.	0.8	3
76	Near-infrared bioluminescence imaging of two cell populations in living mice. STAR Protocols, 2021, 2, 100662.	1.2	2
77	The Monoclonal Antibodies 18d7/91f2 Recognize a Receptor Regulatory Protein on Mouse Bone Marrow Stromal Cells. Journal of Bone and Mineral Research, 2000, 15, 1286-1300.	2.8	1
78	Bone resorption and renal calcium reabsorption in renal cell carcinoma-bearing mice: the effects of bisphosphonate. BJU International, 2007, 99, 1530-1533.	2.5	1
79	Improved Multimodal Tumor Necrosis Imaging with IRDye800CW-DOTA Conjugated to an Albumin-Binding Domain. Cancers, 2022, 14, 861.	3.7	0
80	Investigation of the Therapeutic Potential of Nanobody-Targeted Photodynamic Therapy in an Orthotopic Head and Neck Cancer Model. Methods in Molecular Biology, 2022, 2451, 521-531.	0.9	0